HAL
open science

Anti-Skid Regulation (ASR) of an Electric Vehicle Using Flatness Control

Cédric Chapuis, Xavier Brun, Eric Bideaux, Nicoleta Minoiu-Enache

To cite this version:

Cédric Chapuis, Xavier Brun, Eric Bideaux, Nicoleta Minoiu-Enache. Anti-Skid Regulation (ASR) of an Electric Vehicle Using Flatness Control. 11th International Symposium on Advanced Vehicle Control (AVEC'12), Sep 2012, Séoul, South Korea. hal-00990712

HAL Id: hal-00990712

https://hal.science/hal-00990712v1

Submitted on 30 Apr 2019

HAL is a multi-disciplinary open access archive for the deposit and dissemination of scientific research documents, whether they are published or not. The documents may come from teaching and research institutions in France or abroad, or from public or private research centers.

L'archive ouverte pluridisciplinaire **HAL**, est destinée au dépôt et à la diffusion de documents scientifiques de niveau recherche, publiés ou non, émanant des établissements d'enseignement et de recherche français ou étrangers, des laboratoires publics ou privés.

Anti-Skid Regulation (ASR) of an Electric Vehicle Using Flatness Control

Cedric Chapuis[⋆,⋆⋆], **Xavier Brun**[⋆⋆], **Eric Bideaux**[⋆⋆], **Nicoleta Minoiu-Enache**[⋆]

⋆Renault SAS, 1 avenue du Golf
78288 Guyancourt FRANCE
E-mail: $< firstname > . < name > @renault.com$
⋆⋆Laboratoire Ampere - CNRS : UMR 5005 - Universite de Lyon
Institut National des Sciences Appliquees de Lyon
25 avenue Jean Capelle, F-69621 Villeurbanne Cedex
E-mail: $< firstname > . < name > @insa - lyon.fr$

This paper proposes a flatness based control law for the control of the rear wheels skid of an hybrid vehicle (VELROUE). This vehicle has an ICE[1]traction and an electric propulsion, rear wheels being driven by two independent electric motors. The flatness based control law is here based on a nonlinear two state equations vehicle model, which represents most of the longitudinal dynamics. Firstly, the flat output is identified on the Bond Graph of the vehicle model, then the flat control is designed and is validated in simulation. Finally, this approach is compared to a PI controller classically used in the automotive industry.

Topics/Vehicle Dynamics, Modeling and Simulation, Integrated Chassis Control, Powertrain Control

1. INTRODUCTION

The technical progress as of these last years in the battery field and the strengthening of ecological norms lead to an increasing interest for hybrid and electric vehicles. The emergence of innovative powertrain architectures offers us new opportunities for the control of the vehicles chassis dynamics thanks to power transfer in the powertrain. In this paper, we will consider the ASR[2]. The flatness theory is here used for the design of the ASR function and in a first step, this approach is validated on a virtual vehicle before being tuned on a prototype vehicle from the VELROUE project. VELROUE is a collaborative project subsidized by FEEMA which gathers RENAULT, MICHELIN and IFP. VELROUE's goal is to test a concept of bi-mode powered utility vehicle by developing a demonstrator (Fig. 1). This light utility vehicle is equipped with a front axle powered by an ICE and with two electric motors developed by MICHELIN, clutched to both rear wheels. The developed ASR function enables the control of the rear wheels skid.

The electric motors of VELROUE prototype are controllable in torque. To control this torque and to implement an ASR function, [1] use for instance a linear PID controller fed by the difference between targeted and measured skidding. The wheel-road contact force is computed thanks to a real time differentiation of the rotating wheel speed and a vehicle model similar to the model used later (1). Several techniques based on nonlinear control theory have been applied for the anti-skid. [2] and [3] have used a Model Following Control. [4], [5] and [6] have synthesized first order sliding mode controllers. [4] has applied this control on a vehicle on rail. In these approaches the sliding surface is defined by the difference between desired and measured absolute skidding. [5] has applied this control on a vehicle with a wheel-road contact model based on LuGre model developed in [7]. [6] has developed an ASR function for an electric vehicle. On the contrary to the previous papers, the sliding surface is in this case defined by the difference between the desired and the measured skidding ratio. [8] have studied ASR and

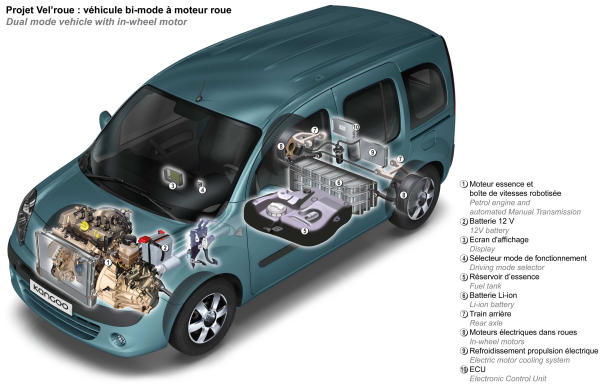

Fig. 1: VELROUE Demonstrator Vehicle

[1]Internal Combustion Engine
[2]Anti-Skid Regulation

ABS[3] with a second order sliding mode control. [9] introduced a fuzzy logic control in order to carry out the ABS function and have used a genetic algorithm to determine in real time the large number of tuning parameters required by the fuzzy logic controller. The authors in [9] have also compared two fuzzy controllers to a linearizing feedback control. The linearizing feedback control was proposed by [10] for the ASR function.
This short review of the literature shows that ASR control laws have been developed for ICE and electric vehicles. In this work the novelty consists in a flatness control, which is applied to an hybrid vehicle with an innovative architecture. The flatness control is developed to control the skidding of the rear wheels driven by two independent electric motors. First the vehicle model used for the synthesis of the controller is described in section 2. A flat output is identified on the Bond Graph representation of the vehicle model. The control law is then synthesized. Simulation results are presented in section 3 before concluding.

2. VEHICLE MODEL AND CONTROL LAW SYNTHESIS

2.1 Vehicle Model

The Bond Graph model (Fig. 3) represents the vehicle model used to synthesize the ASR control. It is based on the "bicycle" model (Fig. 2) that only considers the longitudinal movement and the rotating rear wheel dynamic.

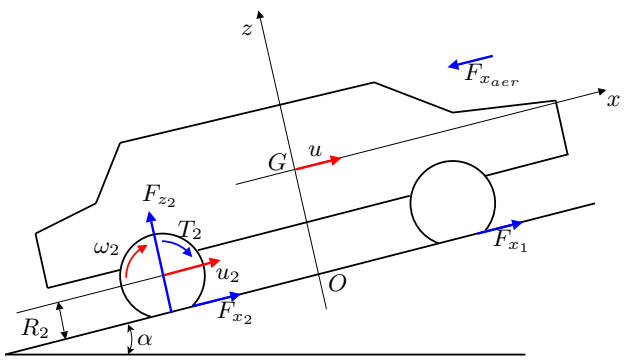

Fig. 2: Vehicle Model Sketch

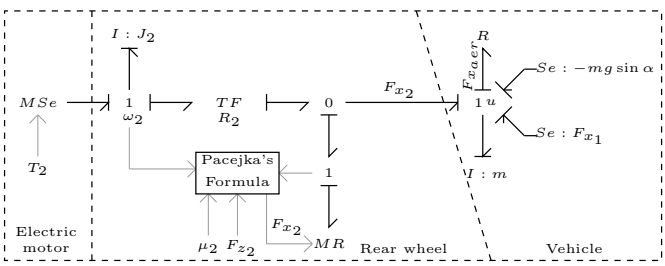

Fig. 3: Bond Graph model for control synthesis

The nonlinear two states equations model (1) corresponds to the Bond Graph representation of the vehicle given in figure 3.

$$\begin{cases} m\dot{u} = F_{x_1} + F_{x_2}(u, \omega_2, F_{z_2}, \mu_2) - F_{x_{aer}}(u) - mg\sin\alpha \\ J_2\dot{\omega}_2 = T_2 - R_2 F_{x_2}(u, \omega_2, F_{z_2}, \mu_2) \end{cases} \tag{1}$$

2.2 Flat Output

To apply the flatness based control design, a flat output is required. This output may be different from the variable to control. In our case, the variable to be controlled, skidding λ_2, is not a flat output. Consequently, the first step of this work aimed at determining a flat output and the requirement for λ_2 need to be expressed with respect to the flat output. A structurally flat output is searched from the Bond Graph (Fig. 3) of the vehicle model described by (1).

Definition 1 (Order of a Bond Graph)**.** *The order of a Bond Graph model is equal to the number of storage elements in integral causality on the Bond Graph in preferential integral causality. It is equal to the number of statically independent variables.*

Definition 2 (Causal path)**.** *On a causal Bond Graph, a causal path links two variable according to the causality of the Bond Graph model.*

Definition 3 (Length of a causal path)**.** *On a causal Bond Graph, the length of a causal path between two variables is equal to the number of integrators (or storage elements in integral causality) encountered along this path.*

Lemma 1 (Structurally flat output identification)**.** *In the case of a nonlinear mono-input system, an output defined by a detector is a structurally flat output if the length of the shortest causal path between this variable and the input of the model is equal to the order of the model.*

Remark 1. *Some singular values may need to reduce the causal path length due to the characteristic relationship of phenomena assuming as in this case the output is no more flat.*

The shortest path between the input T_2 and chassis's speed is represented in figure 4. According to the definition 3, the length of this path is equal to the system's order, that is two. According to the lemma 1, $y_1 = u$ is a structurally flat output of the vehicle model (1).

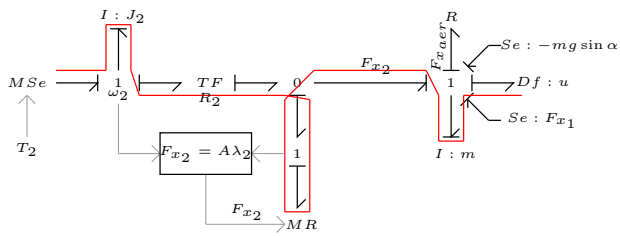

Fig. 4: Structurally flat output

The flatness of the system with respect to the linearizing output found earlier can be verified using

[3] AntiBlockierSystem

the bicausal Bond Graph (Fig. 5) representation of the vehicle model. The order of the inverse model is zero so, the original system is flat [11].

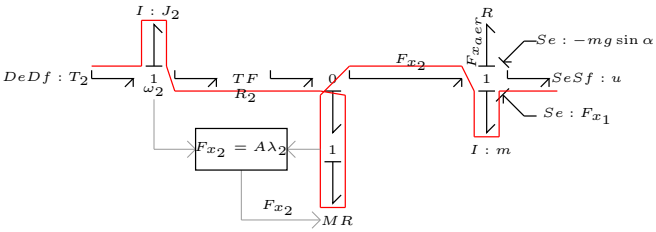

Fig. 5: Causal path on the bi-causal Bond Graph

2.3 Control Law Synthesis

The skidding of the rear wheel λ_2 must be controlled by driving the rear torque T_2. To synthesize the flat control, T_2 must be expressed with respect to the flat output and its derivatives. Flat control is an open loop control law and external disturbances can not be predicted. For instance, the front motor torque T_1, the air resistance force and the influence of the slope of the road are neglected during the flat control design. When the skidding is low, Pacejka's formula for the longitudinal tire force may be approximated by $F_{x_2} = A\lambda_2$ with A constant (Fig. 6) and λ_2 defined by (2).

$$\lambda_2 = \frac{R_2\omega_2 - u}{R_2\omega_2} \tag{2}$$

Whereas the longitudinal tire force F_{x_2} is a function of the adherence coefficient and the vertical force, we consider an average value defined by the usual vehicle live conditions. The vehicle model (1) becomes :

$$\begin{cases} m\dot{u} = A\dfrac{R_2\omega_2 - u}{R_2\omega_2} \\ J_2\dot{\omega}_2 = T_2 - R_2 A\dfrac{R_2\omega_2 - u}{R_2\omega_2} \end{cases} \tag{3}$$

With the structurally flat output identified on the Bond Graph model, it yields :

$$y_1 = u \tag{4}$$

$$y_2 = \dot{y}_1 = \frac{A}{m}\frac{R_2\omega_2 - u}{R_2\omega_2} \tag{5}$$

$$\begin{aligned} U = y_3 = \ddot{y}_1 &= -\frac{A}{m}\left(\frac{\dot{u}\omega_2 - u\dot{\omega}_2}{R_2\omega_2^2}\right) \\ &= -\frac{A}{m}\frac{\dot{u}}{R_2\omega_2} + \frac{A}{m}\frac{u\dot{\omega}_2}{R_2\omega_2^2} \end{aligned} \tag{6}$$

Replacing $\dot{\omega}_2$ by its expression given in (3) enables the expression of the motor torque T_2 to be defined as :

$$\begin{aligned} U &= -\frac{A}{m}\frac{\dot{u}}{R_2\omega_2} + \frac{A}{m}\frac{u}{J_2R_2\omega_2^2}\left(T_2 - R_2A\frac{R_2\omega_2 - u}{R_2\omega_2}\right) \\ T_2 &= \frac{m}{A}\frac{J_2R_2\omega_2^2}{u}U + J_2\omega_2\frac{\dot{u}}{u} + R_2A\frac{R_2\omega_2 - u}{R_2\omega_2} \end{aligned} \tag{7}$$

T_2 must be a function of the flat output y_1 and its derivatives. u may be directly replaced by y_1 but ω_2 needs to be written with respect to y_1 and y_2. From the equation (5) we have :

$$\omega_2 = \frac{y_1}{R_2\left(1 - \dfrac{m}{A}y_2\right)} \tag{8}$$

Then,

$$T_2 = \frac{mJ_2y_1U}{AR_2\left(1 - \dfrac{m}{A}y_2\right)^2} + \frac{J_2y_2}{R_2\left(1 - \dfrac{m}{A}y_2\right)} + R_2my_2 \tag{9}$$

Let us remark that the controller is not defined when $A = 0$ or $A = my_2$. If the wheel is always supposed in contact with the road and if the adherence of the road is supposed never null, the controller is not defined only when $u = 0$. When this specific case occurs, the vehicle's speed is set to a low value close to 0.

As the flatness based controller drives the two dynamics of the system (u, ω_2), it can be assumed that the desired outputs are faithfully followed. In consequence, measured values can be considered equivalent to desired values in the absence of perturbations. The driving torque T_2 may be expressed completely with respect to desired values denoted by $y_i^\star$.

$$T_2^\star = \frac{mJ_2y_1^\star U^\star}{A^\star R_2\left(1 - \dfrac{m}{A^\star}y_2^\star\right)^2} + \frac{J_2y_2^\star}{R_2\left(1 - \dfrac{m}{A^\star}y_2^\star\right)} + R_2my_2^\star \tag{10}$$

The coefficient $A^\star$ such that $F_{x_2}^\star = A^\star\lambda_2^\star$ is needed to compute the torque T_2 (10) to be applied to the rear wheels. The desired skidding $\lambda_2^\star$ is set offline. For control synthesis, A is considered constant for low values of λ_2. The real skidding values may be high, so the coefficient $A^\star$ is computed in real time using Pacejka's representation (Fig. 6) for an adherence coefficient of the road and a vertical force to the wheel which are considered constant (11). This operation must be done online because $\lambda_2^\star$ is specified with respect to the vehicle speed u.

$$A^\star = \frac{F_{x_2}^\star\left(\lambda_2^\star, \mu_0, F_{z_0}\right)}{\lambda_2^\star} = \frac{\phi(\lambda_2^\star)\mu_0F_{z_0}}{\lambda_2^\star} \tag{11}$$

Requirement on the $\lambda_2^\star$ needs to be translated, ie the trajectories of $y_1^\star$ and its derivatives $y_2^\star$ and $y_3^\star$ must be computed from $\lambda_2^\star(u)$. First, $\lambda_2^\star(u)$ is expressed temporarily with respect to the measure of the vehicle speed (Fig. 7).

Once $\lambda_2^\star(t)$ is obtained, the flat output and its derivatives are searched. When the skidding is greater (ie. less) than the desired value, the acceleration of the vehicle needs to be reduced (ie. increased). $y_3^\star$ is $y_2^\star$ derivative and therefore $\dot{u}$ derivative. It represents the time variation of the acceleration (jerk). Therefore, for the ASR function, $y_3^\star$ could be a function of the skidding error e_{λ_2} (12). $y_3^\star$ is integrated to compute $y_1^\star$ and $y_2^\star$ as shown in equations (13) and

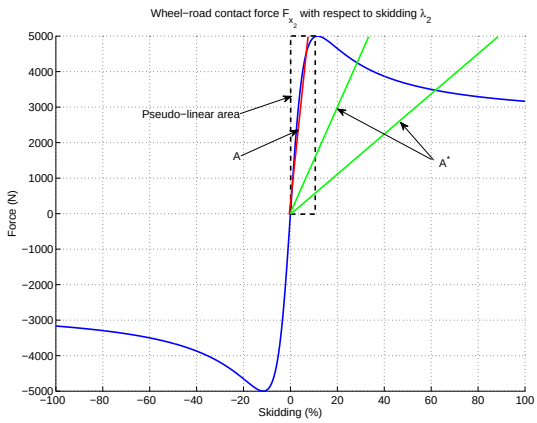

Fig. 6: Pseudo-linear area of Pacejka's representation

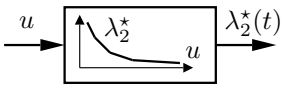

Fig. 7: Transcription of the specifications $\lambda_2^\star(u)$ in a temporal trajectory

(14). The path is planned online because it needs the skidding measure in real time. The acceleration and the desired speed are initialized at each ASR function initialization with the measured values.

$$y_3^\star = K_{y_3} e_{\lambda_2} \qquad K_{y_3} > 0 \tag{12}$$

$$y_2^\star = \int y_3^\star dt \qquad y_2^\star(t_0) = y_2(t_0) \tag{13}$$

$$y_1^\star = \int y_2^\star dt \qquad y_1^\star(t_0) = y_1(t_0) \tag{14}$$

When the open-loop control (10) is applied, the system is equivalent to a double integrator. To ensure its stability, a PI error feedback is implemented. In our case, the goal is not to follow a trajectory formulated in y_1, y_2 and y_3 but to control the skidding. The feedback command is therefore defined from the skidding error e_{λ_2} (16) and not from the flat output and its derivatives. This stabilizing loop is applied to $U^\star = y_3^\star$. The looped system is asymptotically stable outside the singularity $u = 0$. Figure 8 represents the final controller architecture.

$$T_2 = \frac{mJ_2 y_1^\star U}{A^\star R_2 \left(1 - \frac{m}{A^\star} y_2^\star\right)^2} + \frac{J_2 y_2^\star}{R_2 \left(1 - \frac{m}{A^\star} y_2^\star\right)} + R_2 m y_2^\star \tag{15}$$

$$U = y_3^\star + K_p e_{\lambda_2} + K_i \int e_{\lambda_2} dt \tag{16}$$

$$e_{\lambda_2} = \lambda_2^\star - \lambda_2 \tag{17}$$

3. VALIDATION IN SIMULATION

The vehicle model used in simulation to validate the control law considers the six degrees of freedom of the chassis $(x, y, z, \theta, \varphi, \psi)$, the 4 vertical displacements of unsprung masses $(z_{M_{ns}i})$ and the 4 wheels rotations (ω_i). $i = \{1, \cdots, 4\}$. This model consists of five rigid bodies :

- a sprung mass for the chassis and the half axles
- an unsprung mass for each half axles and each wheels.

The simulation model has four wheels whereas the control synthesis model considers only two. A possible approach to overcome this problem is to use a "bicycle" model for the left side of the vehicle and another one for the right side. With this, each side of the vehicle has its own controller.
In the chosen simulation scenario, the vehicle is driving on a flat road with asymmetric adherence. On the left, the adherence coefficient is constant and equals 1, on the right, the coefficient $\mu_{sim}(t)$ varies from 0.2 to 1 (Fig. 9). The rear driving torque asked by the driver $T_{2_{driver}}$ was measured on the VELROUE prototype. It corresponds to an electric start up with full acceleration demand followed by an acceleration release which causes an energy recovery, then an acceleration and another acceleration release (Fig. 10). The front axle driving torque T_1 shown in figure 11 does not match a real use case but it is built to test the stability of the controller in presence of perturbations. This scenario is used to study the influence of a variable and asymmetric estimation error of the adherence coefficient (the adherence coefficient is considered constant in the control law synthesis) in presence of a variable perturbation represented by the contact force at front wheels. The desired skidding $\lambda^\star$ varies slowly with respect to the vehicle's speed.

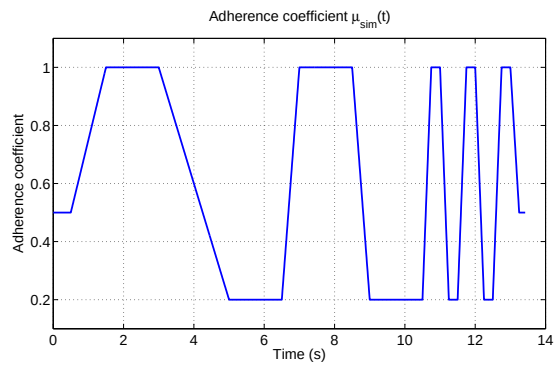

Fig. 9: Variable adherence coefficient $\mu_{sim}(t)$ used for right wheels

Figure 12 illustrates simulation results of the test previously described. The skidding error graph (Fig. 12.d) corresponds to the difference between the measured and desired skidding. When this error is positive, it means that the skidding is excessive. At this moment, the ASR flatness control activates and limits the torque requested by the driver to $T_{2_{ASR}}$. We will particularly pay attention to reduce this error as fast as possible to a negative or null value. Figure 12.b shows the evolution of the adherence coefficient of the road. We are interested in having a look at the response when the adherence coefficient value

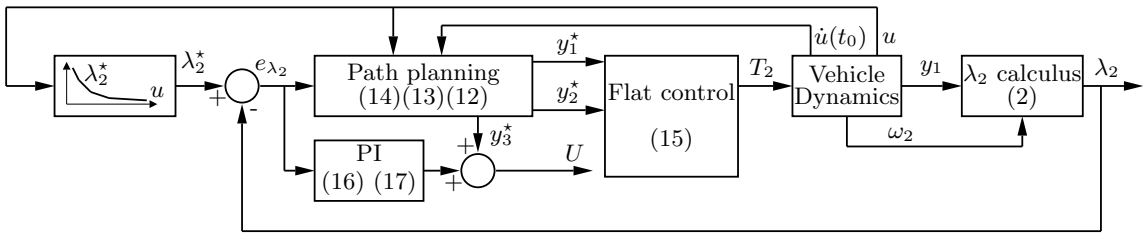

Fig. 8: Flat controller sketch

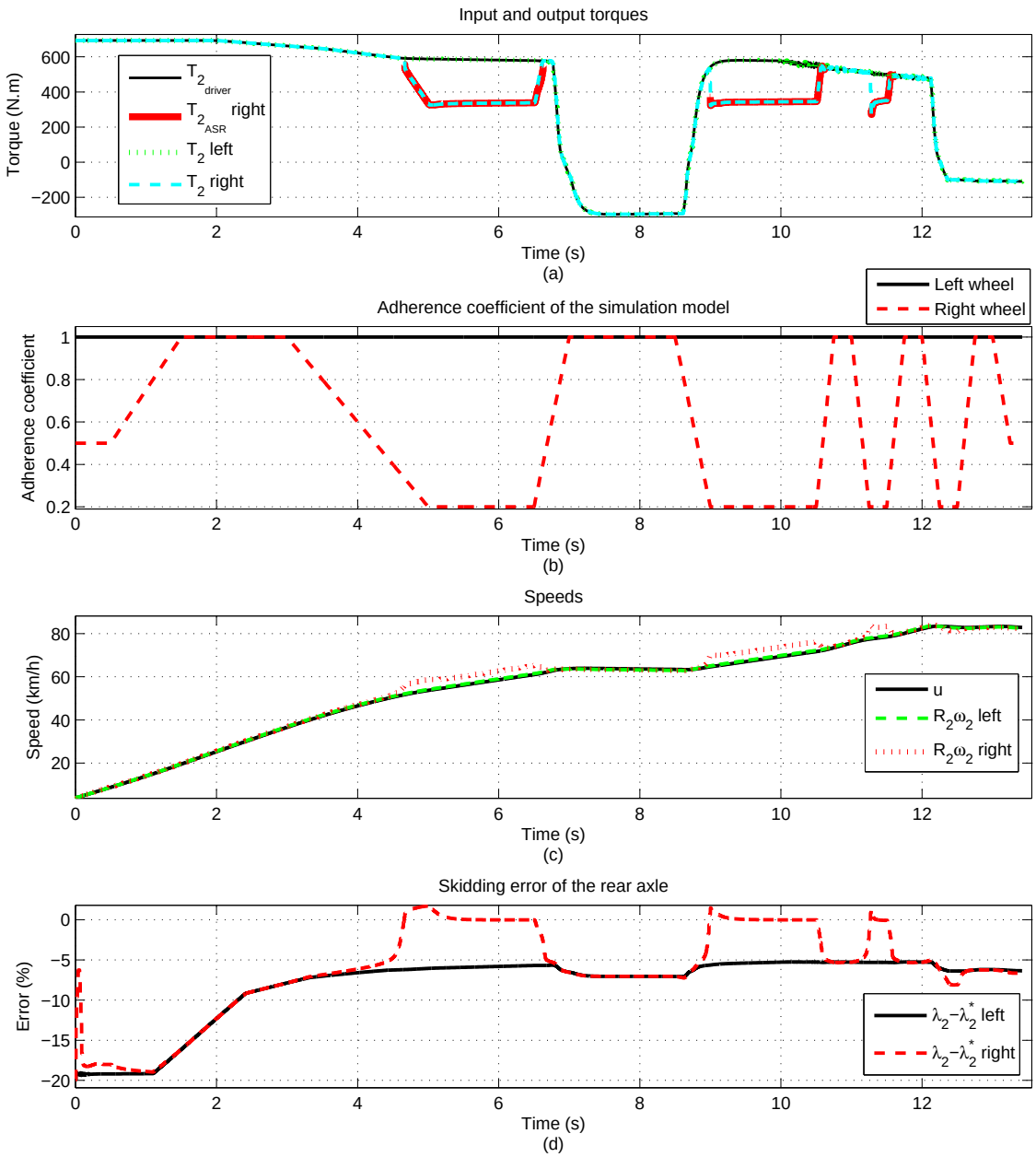

Fig. 12: Simulation results : (a) Rear wheels torques, (b) Adherence coefficients, (c) Speeds, (d) Skidding errors

is low. In these areas, the right rear wheel's speed (dotted line in Fig. 12.c) becomes greater than the left rear wheel's speed (dashed line) and greater than the chassis longitudinal speed (continuous line). The skidding error of the right wheel increases up to 1.7% at $t = 5s$. The ASR control is activated when this error becomes positive. The torque requested by the driver to be applied to the rear wheels (continuous line in Fig. 12.a) is limited by the torque computed by the flat control for the right wheel (bold line). Due to ASR function activation and deactivation, the torque really applied to rear wheels is filtered in

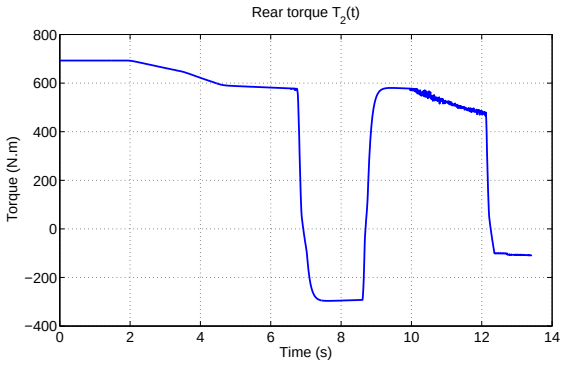

Fig. 10: Rear variable driving torque $T_{2_{driver}}$

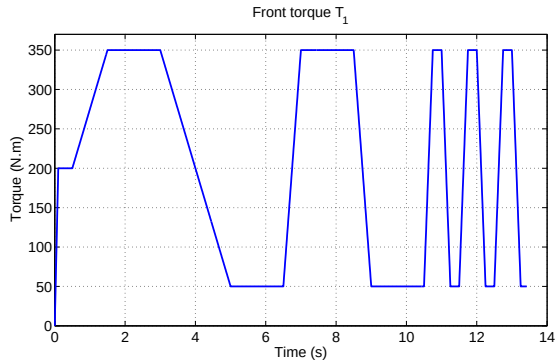

Fig. 11: Front variable driving torque $T_1(t)$

order to avoid too large torque variations during the commutation. This is corresponding to the dotted line for the left wheel and the dashed line for the right wheel. As the two motors are independent, the skidding of each wheel is regulated according to the road adherence on each side (Fig. 12). Consequently, the left wheel can transmit to the road the totality of the torque requested by the driver.
Limiting the maximum transmissible torque at the right wheel produces a torque difference on the rear axle that can lead the driver to correct the vehicle trajectory by a steering action. In cases of extreme asymmetric adherence, when one side of the vehicle is on a surface with almost no adherence, this implementation allows the vehicle to take off by transmitting torque on the wheel of greatest adherence. The right wheel skidding error is reduced and maintained to zero despite a desired skidding out of the pseudo-linear area and external disturbances such as the front driving torque T_1.

4. CONCLUSIONS

In this paper a flat output was identified on the Bond Graph representation of a simplified vehicle model of the VELROUE prototype. A flat nonlinear control was synthesized and validated in simulation. It enables the control of each rear wheel independently. The flat controller is asymptotically stable outside the singularity $u = 0$. The controller tuning is achieved with three parameters, two for the stabilizing loop and one for the path planning. One real time integrator is used in the stabilizing loop and two integrators in the path planning. No instability have been observed during simulations with a variable desired skidding. The control presented in this paper transmits more torque to the road than the PI controller presently used in the VELROUE prototype and it controls properly rear wheels skidding. It improves the vehicle performances during slipping together with driver's comfort. Future works concerning experimental validations with VELROUE vehicle will now be carried out.

5. ACKNOWLEDGMENT

This work comes from a CIFRE PhD (10/169) granted by ANRT in collaboration with RENAULT and the AMPERE LAB. VELROUE project is subsidized by the French Environment and Energy Management Agency. The authors thank MICHELIN, IFP, which are RENAULT partners in this project.

REFERENCES

[1] J. Wang and Q. Wang and L. Jin and C. Song, "Independent wheel torque control of 4WD electric vehicle for differential drive assisted steering", Mechatronics, 2011, Vol. 21, pp. 63-76.

[2] S. Sakai and Y. Hori, "Advantage of Electric Motor for Anti Skid Control of Electric Vehicle", 2000.

[3] D. Yin and S. Oh and Y. Hori, "A Novel Traction Control for EV Based on Maximum Transmissible Torque Estimation", IEEE Trans. On Industrial Electronics, 2009, Vol. 56, No. 6, pp. 2086-2094.

[4] Z. Fan and Y. Koren and D. Wehe,"A Simple Traction Control for Tracked Vehicle", Proc. of the American Control Conference, 1995, Vol. 2, pp. 1176-1177.

[5] C. Canudas and P. Tsiotras, "Dynamic Tire Friction Models for Vehicle Traction Control", Proc. of the 38th IEEE Conference on Decision and Control, 1999, Vol. 4, pp. 3746-3751.

[6] K. Nam and Y. Hori, "Sliding mode controller design for optimal slip control of electric vehicles based on fuzzy vehicle velocity estimation logic", FISITA, 2010.

[7] C. Canudas and H. Olsson and K. J. Astrm and P. Lischinsky, "A new model for control of systems with friction", IEEE Trans. on automatic control, 1995, pp. 419-425.

[8] M. Amodeo and A. Ferrara and R. Terzaghi and C. Vecchio, "Wheel Slip Control via a Second-Order Sliding-Mode Generation", IEEE Trans. On Intelligent Transportation Systems, 2010, Vol. 11, No. 1, pp. 122-131.

[9] F. Chen and T. Liao, "Nonlinear linearization controller and genetic algorithm-based fuzzy logic controller for ABS systems and their comparison", International Journal of Vehicle Design, 2000, Vol. 4, No. 4, pp. 334-349.

[10] T. Nakakuki and T. Shen and K. Tamura, "Adaptive control approach to uncertain longitudinal tire slip in traction control of vehicles", Asian Journal of Control, 2008, Vol. 10, No. 1, pp. 67-73.

[11] P.Y. Richard and J. Buisson and H. Cormerais, "Analysis of flatness using bond graphs and bicausality", Proceedings of the 15th IFAC World Congress, 2002, Vol. 15, No. 1

APPENDICES

e_{λ_2}	rear skidding error
g	acceleration of gravity ($m.s^{-2}$)
m	mass (kg)
u	component of the velocity along x ($m.s$)
A	approximation of Pacejka's representation for low values of λ_2 (N)
$A^\star$	real time approximation of Pacejka's representation (N)
$F_{x_{aer}}$	air resistance force (N)
F_{x_1}	front wheel-road contact force (N)
F_{x_2}	rear wheel-road contact force (N)
F_{z_2}	vertical force on the rear wheel (N)
F_{z_0}	constant vertical force used to compute $A^\star$ (N)
J_2	mass moment of inertia of the rear wheel ($kg.m^2$)
K_i	stabilizing loop integral gain
K_p	stabilizing loop proportional gain
K_{y_3}	proportional gain used to plan y_3 path
R_2	radius of the rear wheel (m)
T_2	rear motor torque (Nm)
$T_{2_{ASR}}$	rear motor torque requested by ASR (Nm)
$T_{2_{driver}}$	rear motor torque requested by the driver (Nm)
α	grade angle of the road (rad)
λ_2	skidding of the rear wheel (%)
$\lambda_2^\star$	desired skidding of the rear wheel (%)
μ_0	constant adherence coefficient used to compute $A^\star$
μ_2	adherence coefficient near the rear wheel
$\mu_{sim}(t)$	variable adherence coefficient used by the simulation model
ω_2	angular velocity of the rear wheel ($rad.s^{-1}$)
$\phi(\cdot)$	normalized Pacejka's representation

Table 1: List of symbols